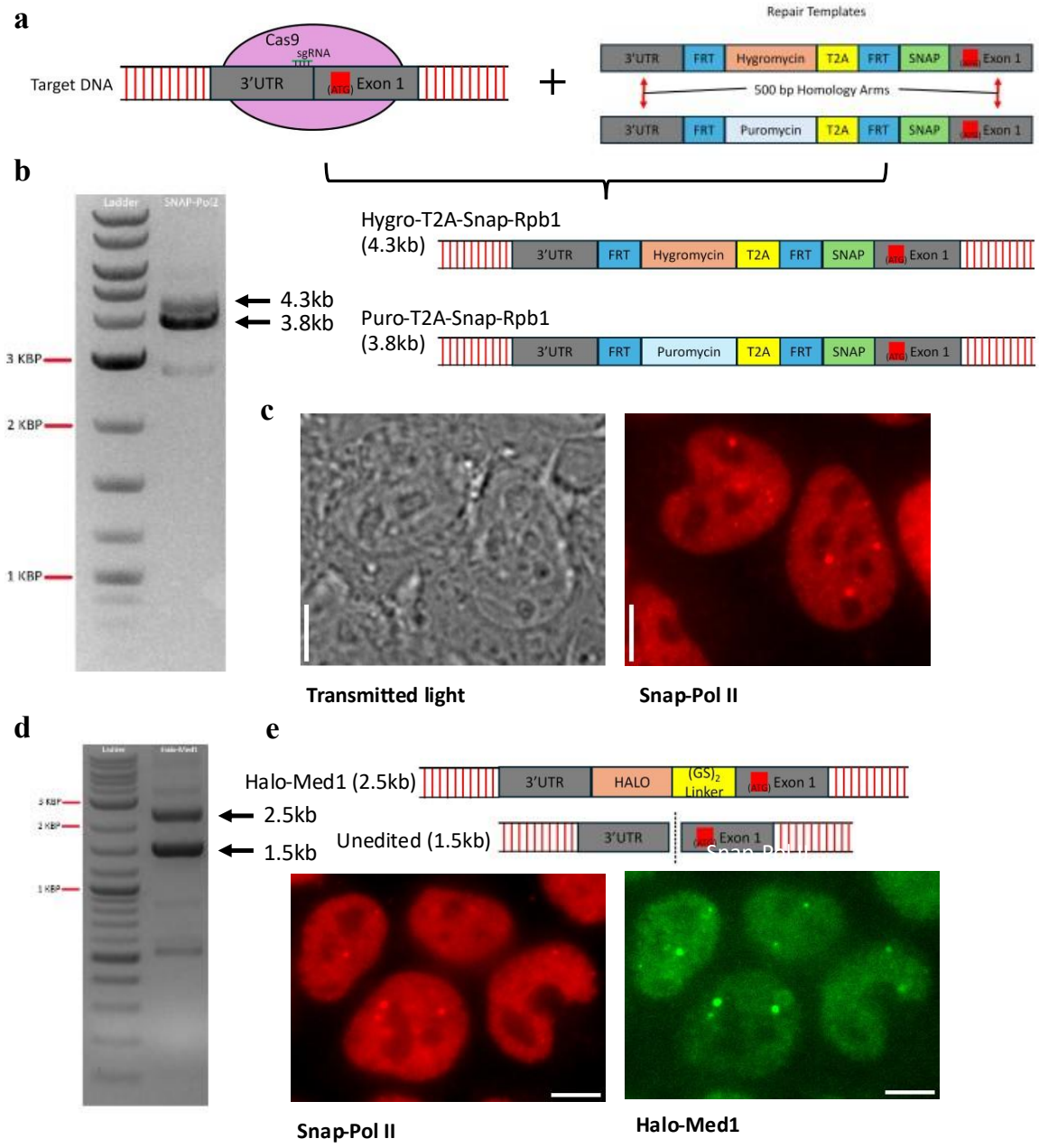

Suppl. Figure 1. Cell line generation. **a)** Schematic representation of CRISPR knock-in. mESCs (V6.5) were transfected with a Cas9 plasmid (PX459 V2.0) comprising a sgRNA template, and a repair template plasmid encoding the insert flanked by 500bp homology arms. To label Pol II, two versions with puromycin and hygromycin selection markers were used to target both alleles. **b**) Insertion in monoclonal cell lines was verified by genomic DNA PCR and both amplicons were sequence-verified for scarless insertion of Snap-Pol II. **c**) Fluorescence image of Snap-Pol2 cell line. Cells were labeled with SnapTag ligand JF-646 (646-Ex/664-Em) **d**) We followed the same approach to create a Halo-Med1 insertion, but omitted antibiotic selection markers. The current cell line carries a homozygous Snap-Pol II edit and a heterozygous Halo-Med1 edit.

a

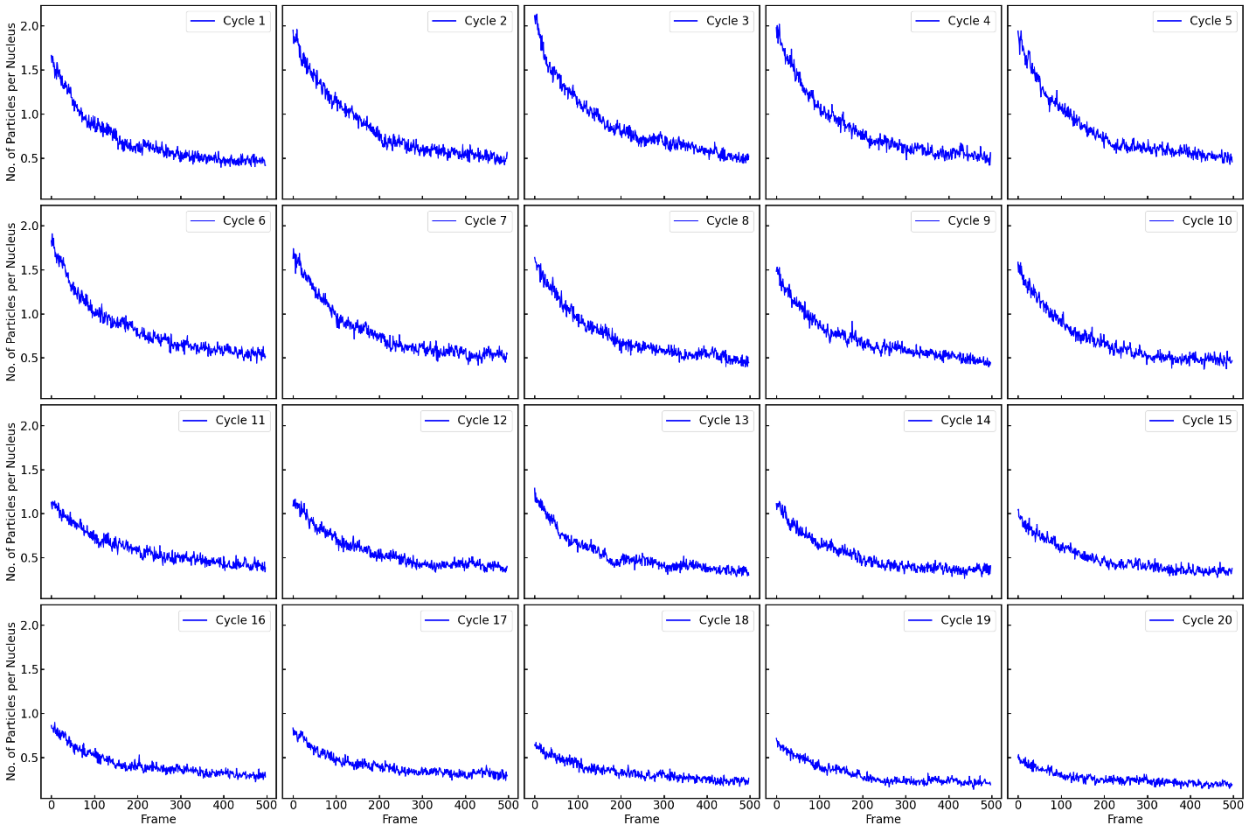

b

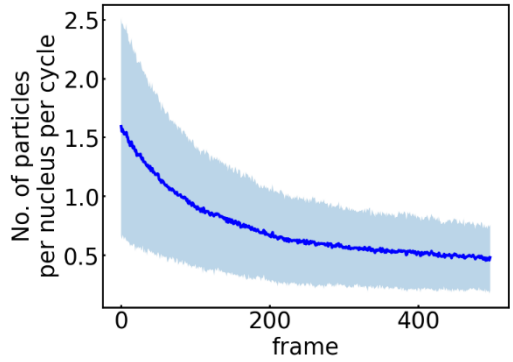

Suppl. Figure 2: Pol II localization rate. a) We used low photo-activation rates to achieve sparse Pol II detections during tracking. Typically, no more than 2 Pol II molecules were detected per frame in a single nucleus. Panels show the detection rate during the 498 frames of each cycle, averaged by cycle number. **b**) Averaged data for all acquisition cycles and nuclei (shaded region represents standard deviation).

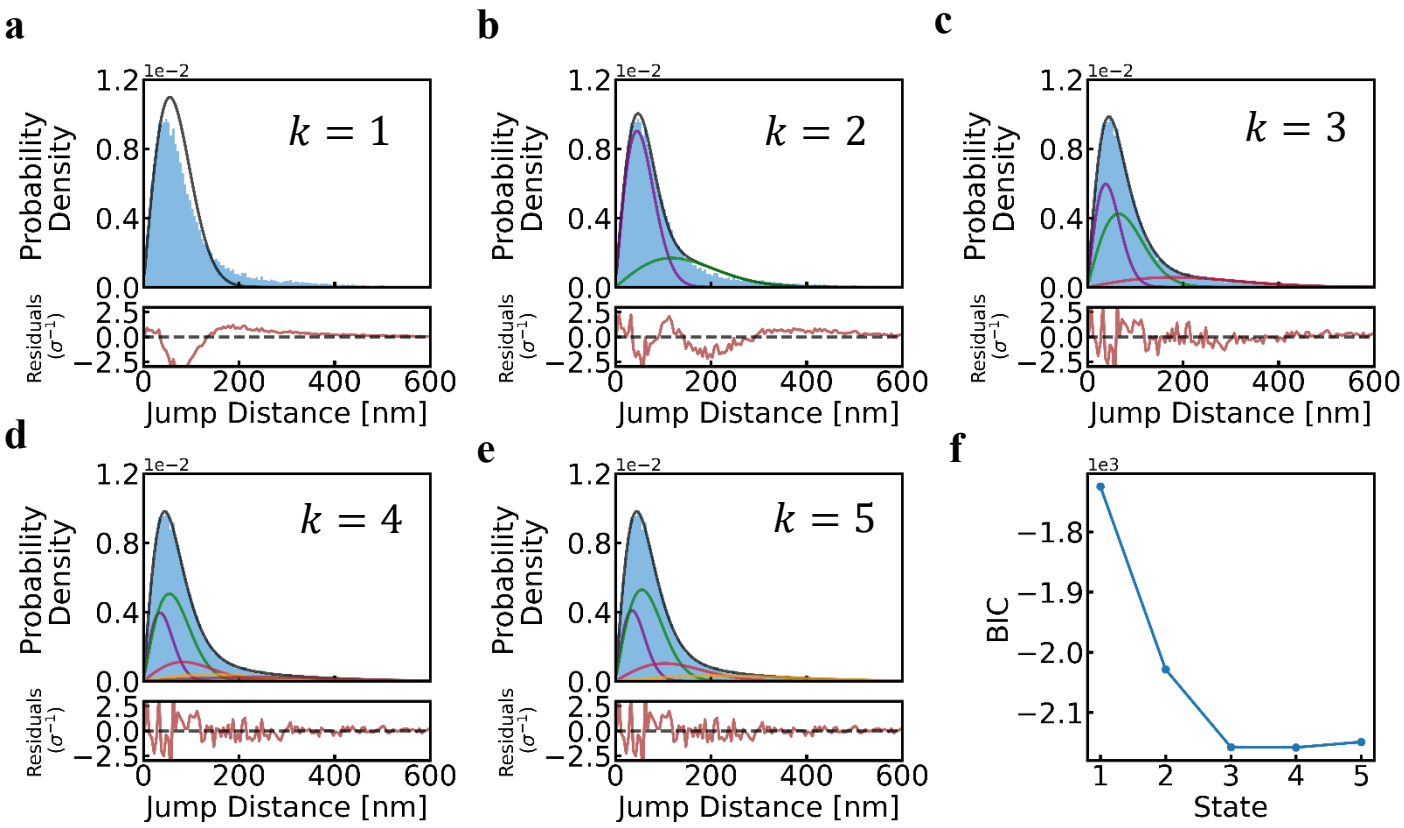

g

# of tracks	128563
# of jumps	476918
# of random sample jumps	25000
# of cells	269
iteration	50

h

Population	f1	f2	f3
D (μm²/s)	0.024 ± 0.007	0.165 ± 0.023	1.535 ± 0.121
Fraction (μ ± s.d.)	37.6 ± 6.35%	45.7 ± 5.27%	16.7 ± 1.23%

Suppl. Figure 3: Pol II has three mobility states inside the nucleus. a-e) Jump distance distribution fit for models with k=1-5 states. f) BIC shows that k=3 is the best fit with minimum score. 25000 jumps were chosen randomly from the full set of 476918 jumps to analyze the jump distance distribution and maintain comparability between conditions and determine confidence intervals. g) Dataset statistics. h) Best fit parameters obtained for the three-state model. Mean and standard deviation of parameters obtained by repeating the random selection of jumps 50 times.

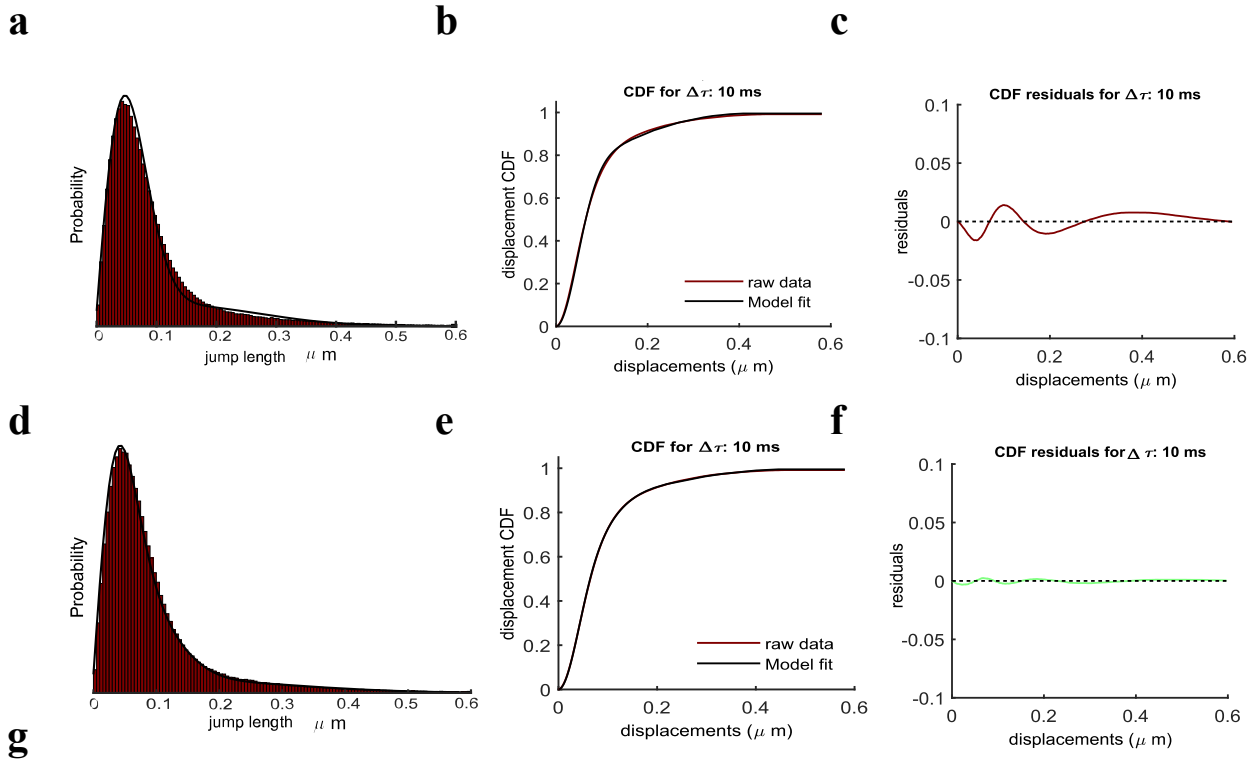

g

Population	f1	f2	f3
D (μm^2/s)	0.03	0.22	1.9
Fraction	43.4 %	39.8 %	16.8 %

Suppl. Figure 4: Spot-On analysis of Pol II mobility. a) Jump distance distribution histogram, **b**) cumulative distribution function, and **c**) residuals for a two-state model fit obtained with the Spot-On tool. **d-f**) Same for a three-state model. The three-state model is a better fit as suggested by our own analysis. **g**) Best fit parameters obtained from Spot-On show close agreement with our model in both diffusion coefficients and relative fractions.

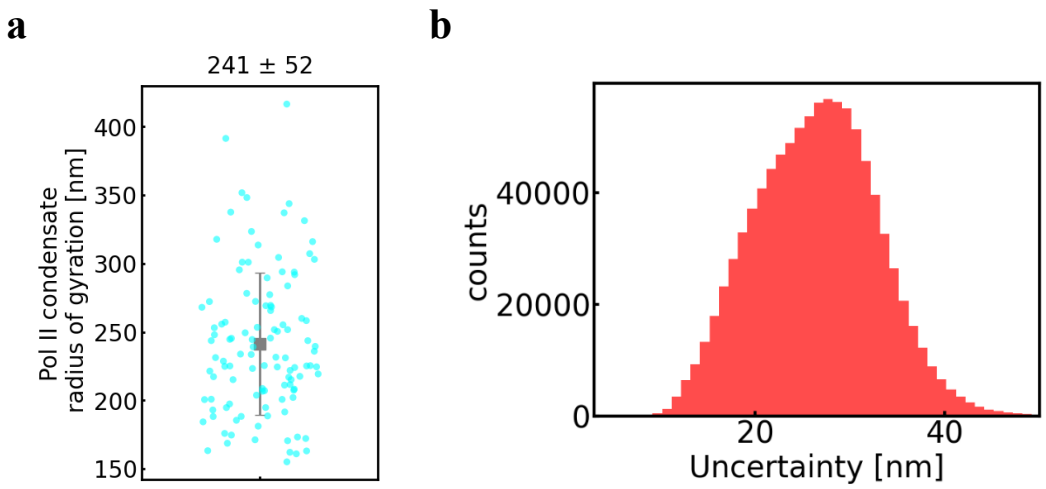

Suppl. Figure 5: Condensate size estimation from super-resolution microscopy. **a**) Radius of gyration calculated for Pol II condensates segmented in super-resolution data using DBSCAN. The mean value of the radius of gyration is 241±52 nm (s.d.) (n=111 condensates). **b**) The distribution of estimated single molecule localization precision for Snap-Pol II obtained from ThunderSTORM during single particle tracking based on the number of detected photons and single molecule signal to noise. Localization uncertainty is substantially smaller (one order of magnitude) than condensate sizes, allowing for single particle tracking inside condensates.

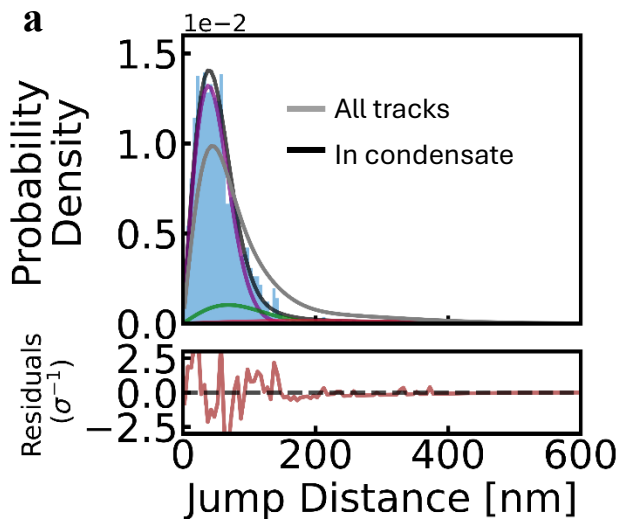

Diffusion coefficient ($\mu \pm$ s.d.) ($\mu m^2/s$)			0.03 $\pm$ 0.01	0.19 $\pm$ 0.03	1.57 $\pm$ 0.11
Condition	**# tracks**	**# jumps**	**F1 ($\mu \pm$ s.d.)**	**F2 ($\mu \pm$ s.d.)**	**F3 ($\mu \pm$ s.d.)**
all tracks (Fig. 1e)	128563	476918	40.8 $\pm$ 0.6 %	44.1 $\pm$ 0.9 %	15.1 $\pm$ 0.5 %
jumps with >= 1 localization inside (this figure)	452	2137	84.0 $\pm$ 2.6 %	11.7 $\pm$ 3.5 %	4.3 $\pm$ 1.2 %
tracks crossing boundary	186	1365	not analyzed		
tracks fully inside (Fig. 2f)	379	1797	88 $\pm$ 2.7 %	8.8 $\pm$ 3.2 %	3.2 $\pm$ 0.9 %
tracks fully inside or crossing boundary	565	3162	78.7 $\pm$ 1.7 %	14.5 $\pm$ 2.2 %	6.8 $\pm$ 0.9 %

Suppl. Figure 6: **Jump distance analysis inside condensates.** Jump distance histogram (blue) of all Pol II displacements with at least one localization inside the condensate volume. This includes tracks fully contained inside condensates and portions of boundary-crossing tracks. Regardless of which criteria are applied, Pol II inside condensate is predominantly in the bound state. For reference, the jump distance distribution for all tracks inside the nucleus is shown in gray, the distribution from tracks fully contained inside condensates is shown in black.

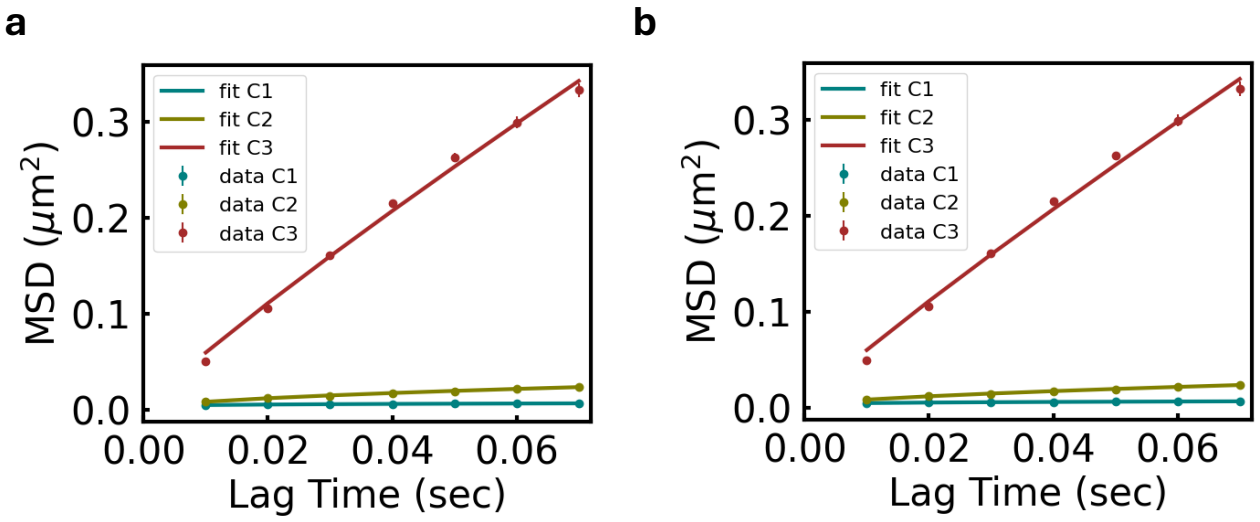

	D (μm^2 /s)	α
C1	0.0025	0.163
C2	0.0246	0.539
C3	0.9355	0.899

	D (μm^2 /s)	α
C1	0.0022	0.2502
C2	0.0282	0.6211
C3	0.954	0.9086

Suppl. Figure 7. Global MSD vs lag time for different components. Fitting with a) $MSD = 4D^{*}t^{\alpha}$ and b) $MSD = 4D^{*}t^{\alpha} + 4\sigma^{2}$, $\sigma = 22nm$. The first seven lag times are considered for fitting.

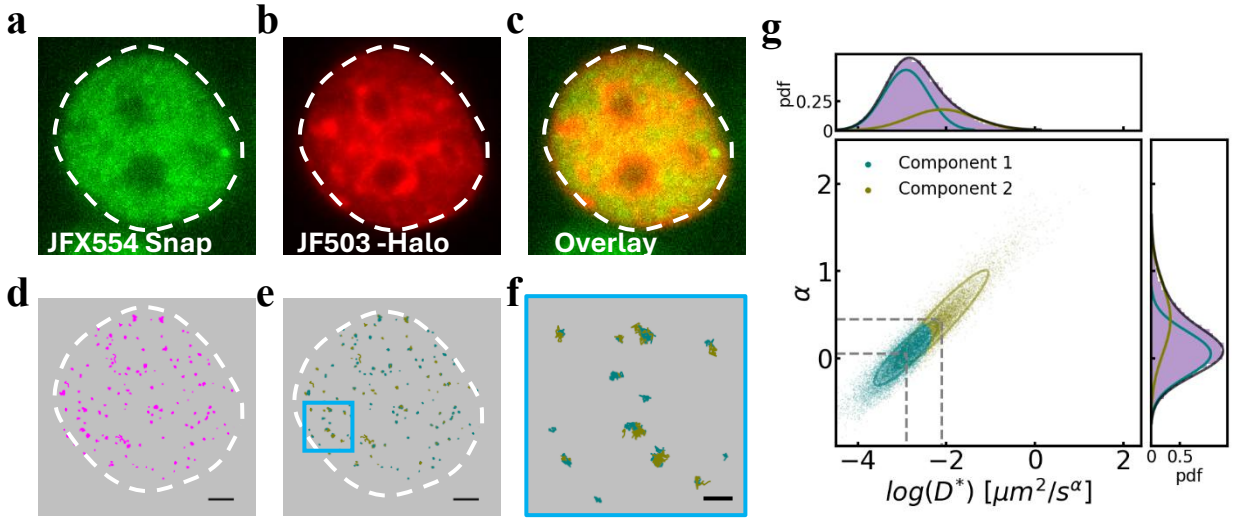

Parameter	Control	TPL
f_1	66.4%	73.3%
α_1	0.054 ± 0.002	-0.020 ± 0.001
$\langle \log(D_1^*) \rangle$	-2.9112 ± 0.0045	-3.1338 ± 0.0021
$\langle D_1^* \rangle\ [\mu m^2/s^\alpha]$	0.0012	0.0007
f_2	33.6%	26.7%
α_2	0.450 ± 0.005	0.295 ± 0.003
$\langle \log(D_2^*) \rangle$	-2.102 ± 0.009	-2.5327 ± 0.0065
$\langle D_2^* \rangle\ [\mu m^2/s^\alpha]$	0.008	0.003

Errors in the tables represent s.e.m calculated.

H2B Untreated: Two independent samples, # of dishes = 2, # of nuclei = 39, # of tracks with length >5 = 18920, # of tracks in component 1 =12587, # of tracks in component 2 = 6333.

H2B TPL: Two independent samples, # of dishes = 5, # of nuclei = 76, # of tracks with length >5 = 63477, # of tracks in component 1 = 45918, # of tracks in component 2 = 17559.

Suppl. Figure 8: H2B single particle tracking a) Two-color imaging of Snap-Pol II (JFX554) and **b**) H2B-Halo (JF503). **c**) Overlay. **d**) We tracked single H2B-Halo molecules labeled with PA-JF646. **e**) Tracks color-coded according to populations identified in a Gaussian mixture model analysis of an α – log(D) histogram. **f**) Zoomed-in view of the area highlighted in blue. **g**) α vs log (D^*) histogram obtained from H2B-Halo single trajectory MSD analysis. The best description based on BIC scores is a two mobility state model. Component 1 (teal) is immobile with a 66.4% fraction, Component 2 (yellow) is sub-diffusive with a 33.6% fraction. TPL treatment shows only minimal effects on H2B mobility (Table). Scale bars a) 2 µm f) 500nm.

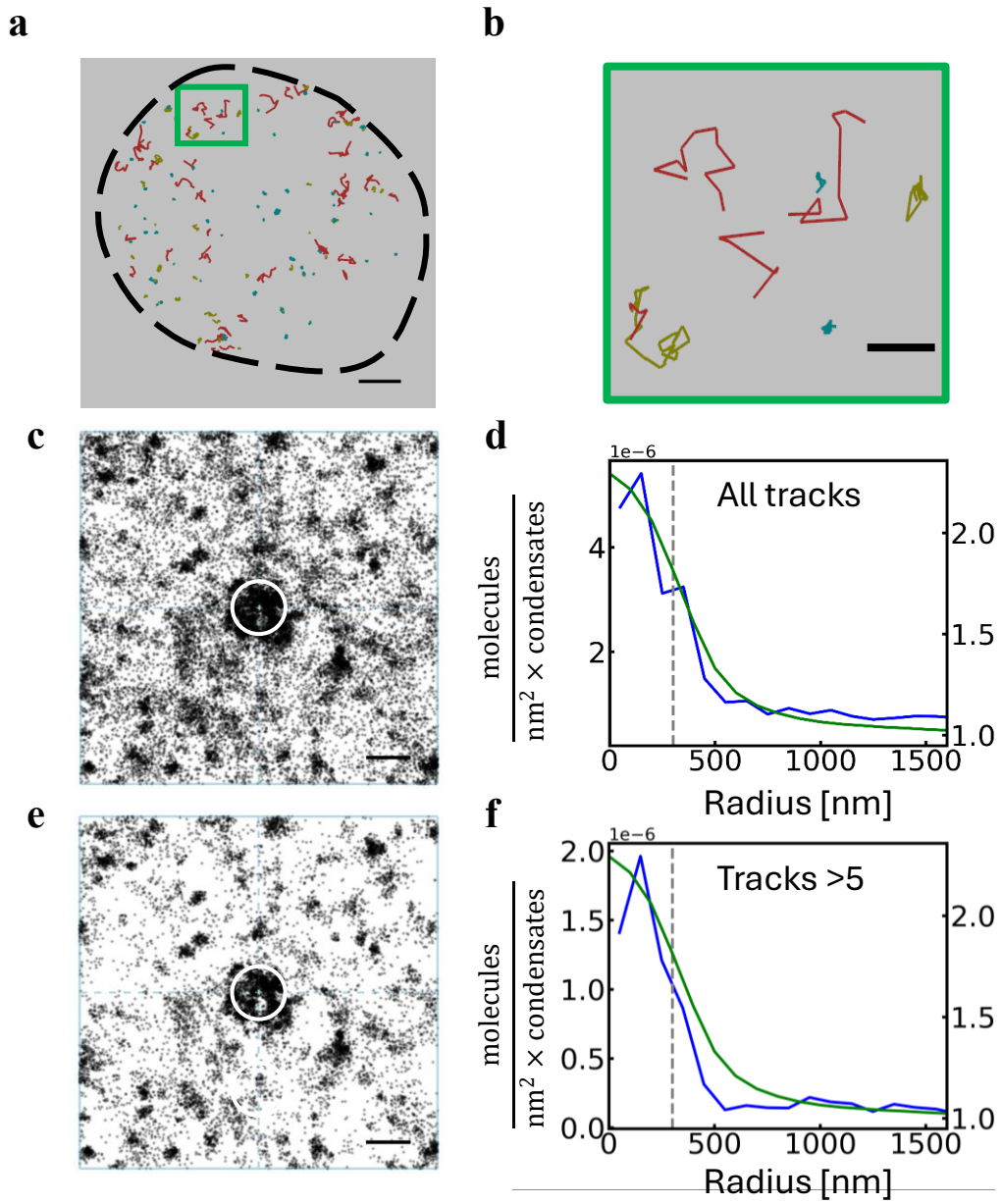

radius	mol / (nm^2 x condensates) (all tracks)	mol / (nm^2 x condensates) (length >5)
0-300 nm	$40.6 * 10^{-7}$	$14.8* 10^{-7}$ (36%)
300-700 nm	$15.3 * 10^{-7}$	$3.1 * 10^{-7}$ (20%)
700-1500 nm	$8.0 * 10^{-7}$	$1.6 * 10^{-7}$ (20%)
enrichment factor	40.6/8.0 = 5.13	14.8/1.6 = 9.2

Suppl. Figure 9: Single track MSD analysis. a) Pol II tracks in a single nucleus (black dashed line) color-coded by the state determined from a Gaussian mixture model analysis of the α vs $\log^*(D)$ histogram. Tracks from the bound component 1 (teal), sub-diffusive component 2 (yellow), and diffusive component 3 (red) are distributed throughout the nucleus. **b**) Zoomed-in view of the area highlighted in green. (Scale bar a) 2 µm b) 500nm). For single track MSD analysis, we consider only tracks with length >5. To assess the impact of dropping shorter, typically higher mobility tracks on apparent enrichment factors we compare c) Pol II localizations from all tracks aligned w.r.t to condensate centers and d) the radial track density to tracks with length > 5 considered in single track MSD analysis (e,f). The enrichment factor increases for the longer tracks because more short (mobile) tracks are dropped outside condensates at radii >300nm. This further emphasizes that Pol II in condensates is bound.

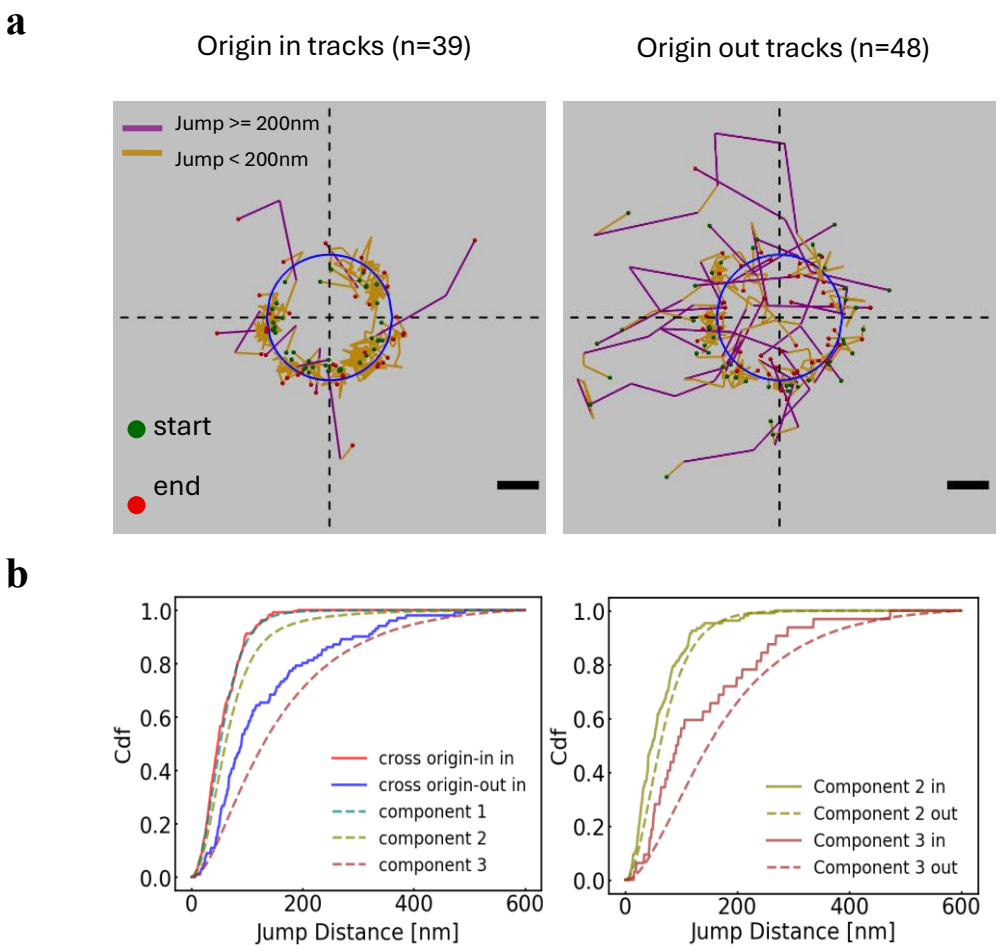

Suppl. Figure 10: Crossing tracks analysis. We observed few tracks crossing the condensate boundary. To exclude ambiguous tracks located at the designated radial cutoff (300nm), we exclude tracks situated in a buffer zone (+- 20nm). Tracks are considered 'origin inside' (n=39) and the first localization occurred at <280nm radius and at least one localization was detected at >320nm. Similarly, 'origin outside' tracks (n=48) have the first localization at >320nm radius and at least one subsequent localization at <280nm. We plotted these tracks separately and color-coded jumps by mobility. **a**) 'Origin in' tracks (left) are of low mobility, concentrated towards the condensate surface, and show only rare long jumps mostly outside the condensate. 'Origin out' tracks (right) show a larger fraction of long jumps (>200nm) and traverse the condensate volume. 58% of 'origin out' tracks end inside the condensate, 15% in the border zone, only 27% end outside the 320nm radius. **b**) Mobility of tracks inside condensates (left). Jumps inside the condensate of 'origin in' tracks (red) have the same mobility as the bound component 1 tracks (teal dashed) classified by single track MSD analysis. The inside portion of 'origin out' tracks after crossing into the condensate (blue) has a much higher mobility approaching the freely diffusive component 3 (orange dashed). (right) Vice versa, jumps from subdiffusive tracks (component 2, yellow) have similar mobility inside (solid) and outside (dashed) condensates, whereas jumps from freely diffusive tracks (orange, component 3) indicate slightly reduced mobility inside condensates (solid) as compared to outside (dashed). Scale bar **a)** 200nm.

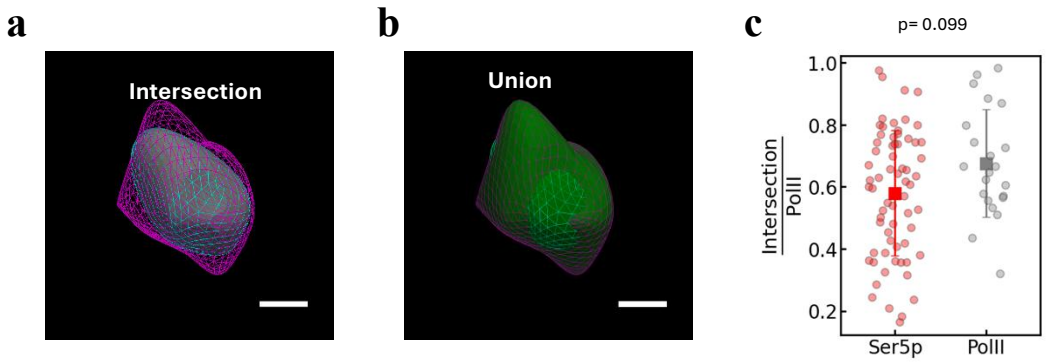

Suppl. Figure 11 Overlap fraction analysis a) Intersection and b) union of condensate volumes segmented in the two color channels independently. c) Overlap fraction quantified as intersection volume divided by segmented volume in the general Pol II channel for imaging of Ser5p-PolII/Pol II (red) and two-color Pol II-Pol II (gray) using the same dye combinations. Overlap of Ser5p-Pol II with general Pol II is not significantly different than two-color Pol II-Pol II overlap. (Wilcoxon sum rank test.) Scale bar a,b) 200nm.

a

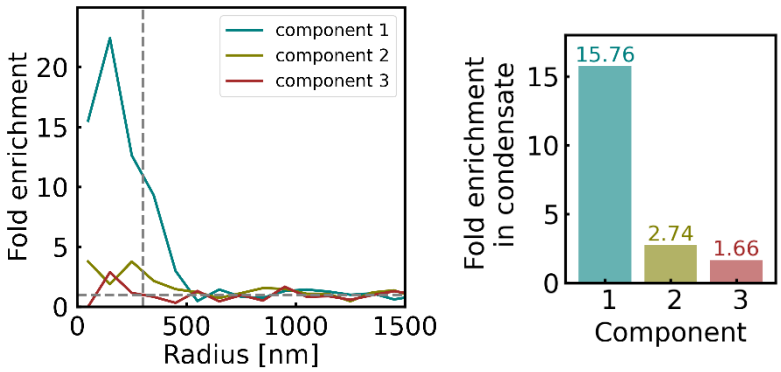

radius	Mol per nm^2 per condensates (component 1)	Mol per nm^2 per condensates (component 2)	Mol per nm^2 per condensates (component 3)
0-300 nm	137.4 * 10^{-8}	15.0 * 10^{-8}	5.8 * 10^{-8}
300-700 nm	24.6 * 10^{-8}	6.1 * 10^{-8}	2.6 * 10^{-8}
700-1500 nm	8.7 * 10^{-8}	5.5 *10^{-8}	3.5 * 10^{-8}
Enrichment factor	137.4/8.72 = 15.76	14.98/5.47 = 2.74	5.84/3.52 = 1.66

b

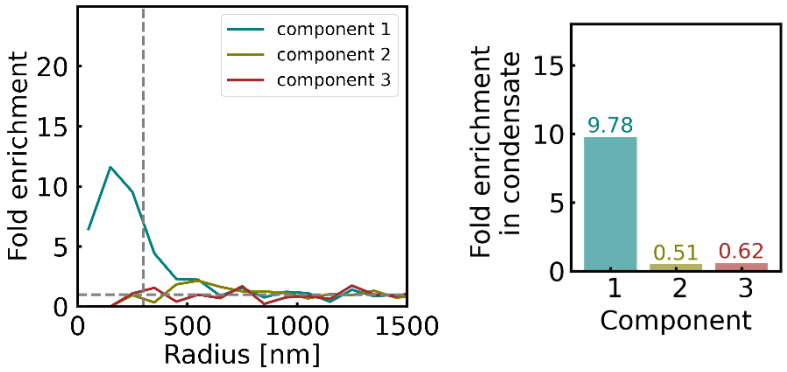

radius	Mol per nm^2 per condensates (component 1)	Mol per nm^2 per condensates (component 2)	Mol per nm^2 per condensates (component 3)
0-300 nm	456.1* 10^{-8}	1.29 * 10^{-8}	1.95 * 10^{-8}
300-700 nm	101.1 * 10^{-8}	3.92 * 10^{-8}	2.78 * 10^{-8}
700-1500 nm	46.7* 10^{-8}	2.51*10^{-8}	3.16 * 10^{-8}
Enrichment factor	456.1/46.7=9.78	1.29/2.51=0.51	1.95/3.16=0.62

Suppl. Figure 12: Condensate enrichment of different mobility components. a) Untreated control and b) TPL-treated cells (30 mins). We determined track densities in different radial regions around condensates centers. Fold enrichment in 100nm intervals is plotted as track density relative to a control region at radius 700 – 1500nm. The enrichment factor is calculated as the ratio of track density inside condensates (<300nm radius) over track density in a control region (700-1500nm radius). The immobile component 1 is most highly enriched inside condensates. Components 2 (subdiffusive) and 3 (freely diffusive) show weak enrichment (untreated) or depletion (TPL).

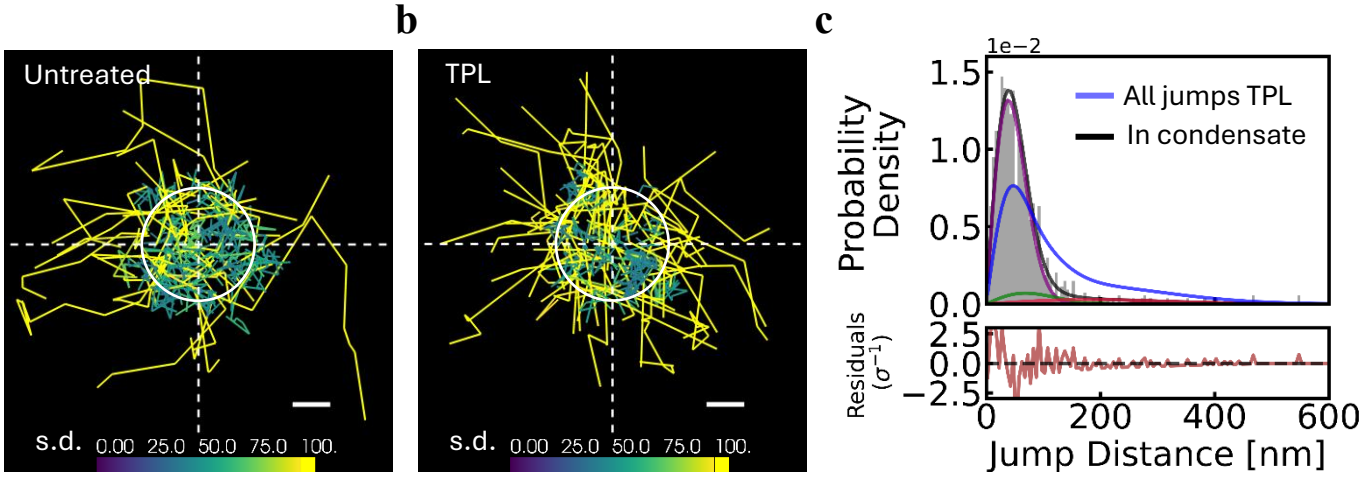

Diffusion coefficient ($\mu \pm$ s.d.) ($\mu m^2/s$)			0.03 $\pm$ 0.01	0.19 $\pm$ 0.03	1.57 $\pm$ 0.11
Condition	**# tracks**	**# jumps**	**F1 ($\mu \pm$ s.d.)**	**F2 ($\mu \pm$ s.d.)**	**F3 ($\mu \pm$ s.d.)**
all tracks (Fig. 5a)	77763	228915	27.3% $\pm$ 0.8 %	38.7% $\pm$ 1.0 %	34.0% $\pm$ 0.6 %
jumps with >= 1 localization inside (this figure)	284	1074	83.7% $\pm$ 3.26 %	8.0% $\pm$ 4.2 %	8.3% $\pm$ 1.4 %
tracks crossing boundary	138	740	not analyzed		
tracks fully inside (Fig. 5b)	226	877	88.5% $\pm$ 3.7 %	7.5 % $\pm$ 4.6 %	4.0%1.5 %
tracks fully inside or crossing boundary	364	1617	75.5% $\pm$ 2.6 %	13.0% $\pm$ 3.3 %	11.5% $\pm$ 1.3 %

Suppl. Figure 13: TPL causes an increase in mobility of Pol II inside condensates. To assess the impact of TPL treatment on mobile Pol II inside condensates we removed all tracks with coordinate standard deviation >40nm. **a**) Mobile Snap-Pol II tracks aligned by condensates center for untreated and **b**) TPL-treated conditions color-coded by mobility. Under TPL treatment, more mobile tracks (yellow) traverse the condensate. **c**) Jump distance distribution for all jumps inside the nucleus (fully contained tracks and inside portion of crossing tracks) under TPL-treatment (black) compared to the distribution of all jumps under the same condition (blue). **d**) Comparison of mobility fractions in different subsets of tracks under TPL treatment. Compare **Suppl. Fig. 6** for untreated condition.

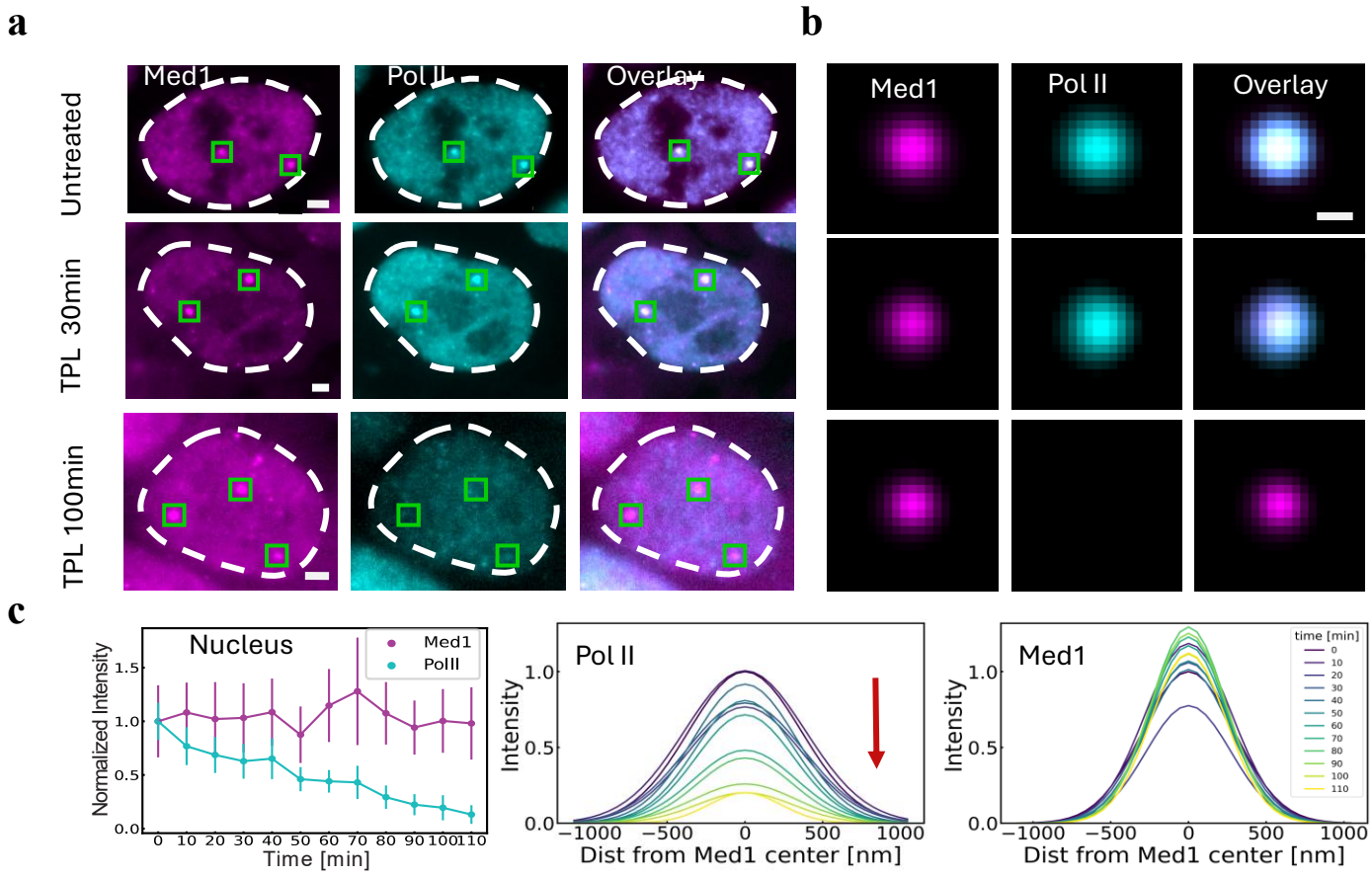

Suppl. Figure 14: Initiation inhibition leads to Pol II degradation. a) Two-color imaging of Halo-Med1 (TMR) and Snap-Pol II (JF646) at different time points after triptolide addition: untreated (top), 30 mins incubation(middle), and 100 mins incubation (bottom). b) Overlay of signal from Pol II (cyan) and Med1 (magenta) channels at condensate positions identified in the Med1 channel. Compared to untreated cells (top, n=38 condensates), Pol II is only slightly degraded after 30 min TPL incubation (middle, n=53 condensates). Long incubation for 100 mins strongly degrades Pol II (bottom, n=79 condensates). Condensates persist in the Mediator channel (magenta). c) The measured intensity of Med1 normalized to the untreated condition is constant, while Pol II intensity is diminished over time after TPL addition in the whole nucleus. d) Pol II intensity in condensates gradually decreases to the same degree, while Mediator intensity shows little variation. Tracking experiments were conducted at early time points up to 30mins after TPL addition. Scale bar: a) 2 µm b) 500nm.

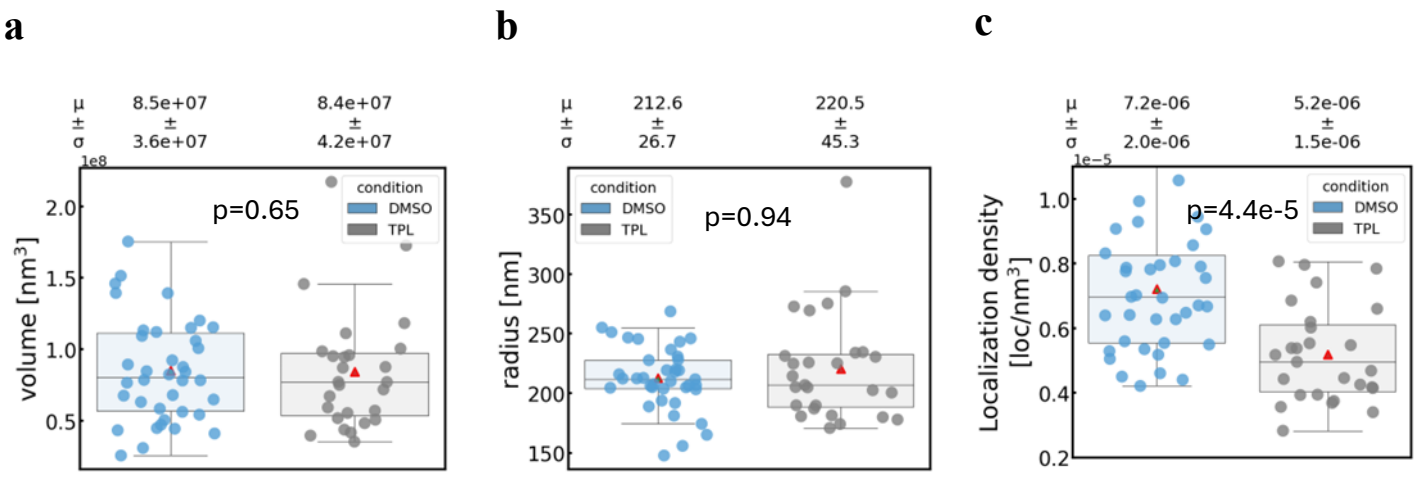

Suppl. Figure 15: The size and volume of Pol II condensates are not affected by 30-minute triptolide treatment. a) Volume, b) radius of gyration, and c) localization density for Pol II. Condensate volumes obtained by DBSCAN segmentation of two-color super-resolution images in control (DMSO, blue) and TPL treatment (gray) conditions. Pol II localization density is reduced by ~30% (p=4.4e-5) in agreement with widefield intensity measurements, but condensate volume and radius do not change. Two-sided Wilcoxon rank-sums test.

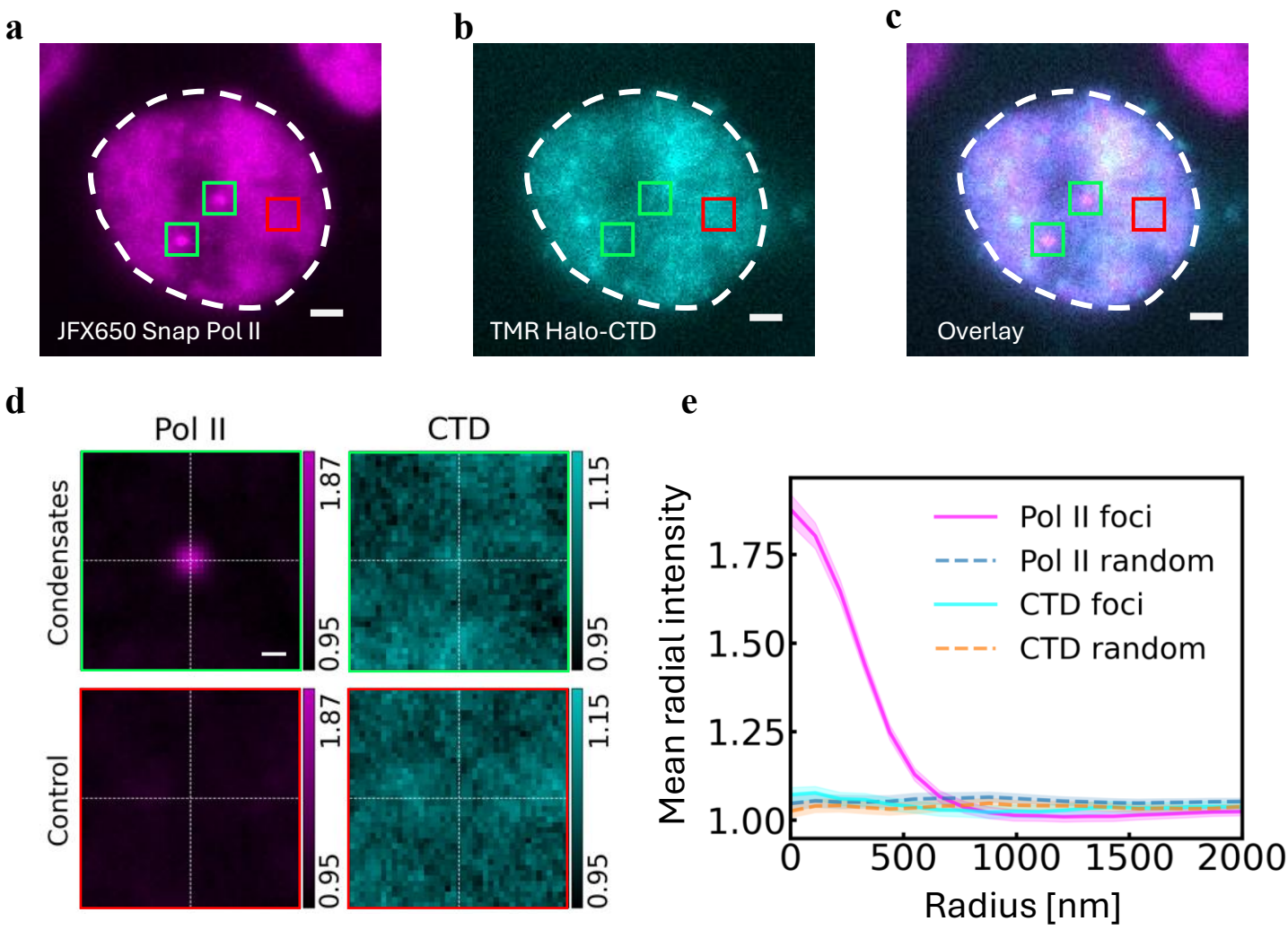

Suppl. Figure 16: CTD is minimally enriched in Pol II condensates (fixed cell data). a) Two-color imaging of Snap-Pol II (JFX650) and b) Halo-CTD (TMR) in fixed cells. c) Overlay of both channels. Green squares represent identified condensates. Red square denotes randomized control region. d) Top: Overlay of signal from both channels accumulated at n=84 Pol II condensates from 66 fixed cells. Halo-CTD signal (top right) at Pol II condensates (top left) shows weak accumulation. Bottom: Overlay of signal at an equal number of randomized coordinates in the nucleus. e) Mean radial intensity plots for accumulated signal shown in d). CTD signal weakly accumulates in condensates in fixed cells. Scale bar a-c) 2 µm, d) 500nm).

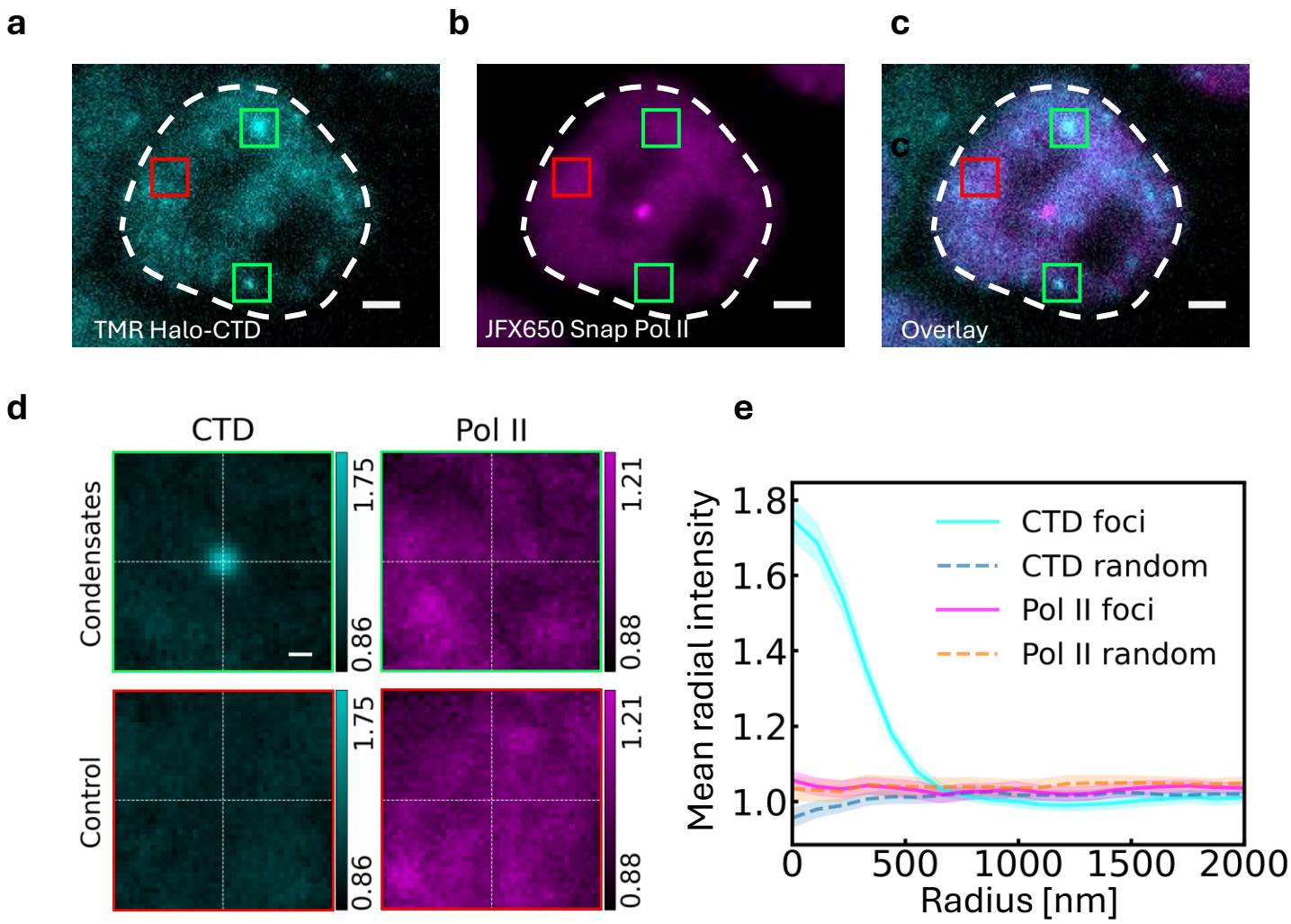

Suppl. Figure 17: Pol II is not enriched in CTD foci a) Two-color imaging of Halo-CTD (TMR) and b) Snap Pol II (JFX650). c) Overlay of both channels. d) Top: Overlay of signal from both channels accumulated at n=39 Halo-CTD foci from 31 cells. Snap-Pol II signal (top right) at CTD foci (top left) shows no accumulation. Bottom: Overlay of signal at an equal number of randomized coordinates in the nucleus. e) Mean radial intensity plots for accumulated signal shown in d). Pol II signal does not accumulate in CTD foci. Scale bar a-c) 2 µm, d) 500nm).

Supplementary Tables

Suppl. Table 1: Primer sequences.

Purpose	Sequence	Type	Purpose
Med1 CRISPR	5'-TGTCTGCTGGGATCAAAGGCTT-3'	Forward	gDNA amplification of left homology arm
	5'-AGCCTTCATCCTGACAGCCGGG-3'	Reverse	
	5'-AGGGGGAAACCGAGGGTG-3'	Forward	gDNA amplification of right homology arm
	5'-GCAGTTCGTAAAGACACAGCAC-3'	Reverse	
	5’-CACCGCTCTCTTGATGGTGCGCAGC-3'	Forward	sgRNA insertion into px459v2.0
	5’- AAACCCTGAGCCTTCATCCTGACAC -3'	Reverse	
Pol II CRISPR	5'-CCGAGAGCGCGACCGGGAC-3'	Forward	gDNA amplification of left homology arm
	5'-GGCGAGGCAGGCGCGCTG-3'	Reverse	
	5'-ATGCACGGGGGTGGCCCC-3'	Forward	gDNA amplification of right homology arm
	5'-TTCCTAGTGTCTGATTACTG-3'	Reverse	
	5’-CACCGCTCTCTTGATGGTGCGCAGC-3'	Forward	sgRNA insertion into px459v2.0
	5’- AAACGCTGCGCACCATCAAGAGAGC -3'	Reverse	
H2B-HaloTag Cloning	5’-TTCCGGCTCCGGCGACAGCGGCGTG-3'	Forward	H2B-D2 Backbone amplification
	5’-CTGCCATGGTGGCGACCGGTGGATCC-3'	Reverse	
	5’-ATGGCAGAAATCGGTACTGG-3'	Forward	HaloTag amplification
	5’-GCCGGAAATCTCGAGCGTC-3'	Reverse	
HaloTag-CTD Cloning	5’-CCTATAGGTGGTGCTATGTCTCC-3'	Forward	gDNA amplification of Pol2-CTD
	5’-CTTCGCCCTGTTCGCTCAG-3'	Reverse	

Suppl. Table 2: Antibodies used for immunofluorescence staining in dSTORM microscopy.

Primary antibodies					
Target (epitope)		**Host species**	**Source**	**Cat. No.**	**Dilution**
RNA Pol II		Rabbit	Abcam	ab26721	1:500
RNA Pol II		Mouse	Santa Cruz Biotech	Sc47701	1:500
Ser5p Pol II		Mouse	MBL	Mabi 0603	1:100
Secondary antibodies					
Target (epitope)	**Label**	**Host species**	**Vendor**	**Cat. No.**	**Dilution**
Mouse	AF488	Donkey	Abcam	ab150105	1:500
Rabbit	AF647	Donkey	Abcam	ab150075	1:500
Experiment	**1º**	**2º**	**1º**	**2º**	
Pol II + Ser5p	ab26721	ab150075	Mabi 0603	ab150105	
Pol II + Pol II	ab26721	ab150075	Sc47701	ab150105	

Suppl. Table 3: Fluorescent probes for endogenous protein labeling

Fluorophore	**Source**	**Final concentration**	**Purpose**
PAJF646 Snap	Luke Lavis, HHMI Janelia Research Campus	120nM	Pol II tracking
JFX554 Snap	Luke Lavis, HHMI Janelia Research Campus	50nM	Pol II reference labeling
JFX650 Snap	Luke Lavis, HHMI Janelia Research Campus	50nM	Pol II reference labeling
PAJF646 Halo	Luke Lavis, HHMI Janelia Research Campus	120nM	H2B-Halo, CTD-Halo tracking
JF549 Snap	Luke Lavis, HHMI Janelia Research Campus	500nM	Pol II reference labeling
Halo TMR	Promega	200nM	Mediator reference labeling
JF503 Halo	Luke Lavis, HHMI Janelia Research Campus	500nM	H2B-Halo, CTD-Halo reference labeling

Supplementary Videos

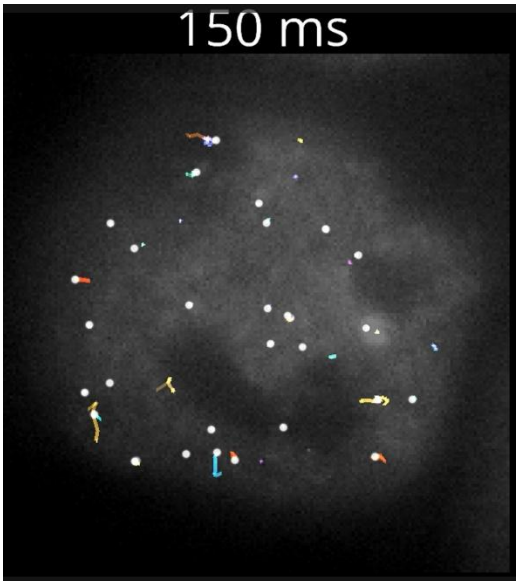

Video S1. Single PAJF646-Snap-Pol II tracks in a live cell acquired at 10ms frame interval, related to Figure 1. Tracks recorded in all 15 acquisition cycles for this cells were overlaid on the JFX554-Snap-Pol II reference image.

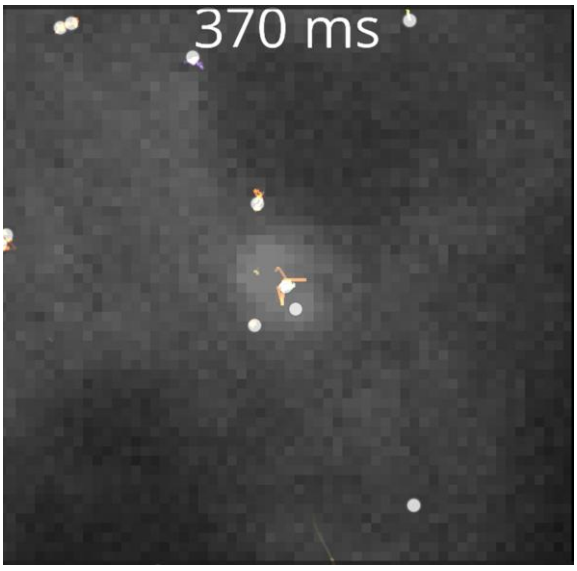

Video S2. Snap-Pol II tracks acquired at a condensate identified in a single cell, related to Figure 2a. Zoomed-in view of Video S1 centered on a condensate region.

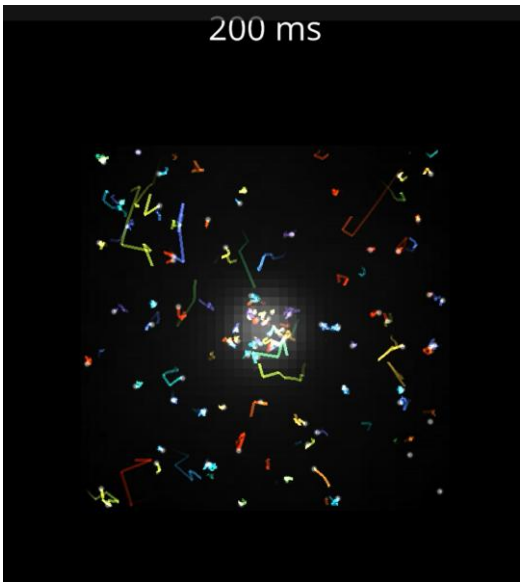

Video S3. Snap-Pol II tracks at condensates accumulated from all cells and acquisition cycles, related to Figure 2b.